The Role of Melting on Intimate Contact Development in Laser-Assisted Tape Placement of Carbon Fibre Reinforced Thermoplastic Composites

Jimenez del Toro, A.; Teuwen, Julie J.E.; Tomás, Flanagan ; Finnegan, William

Citation (APA)
Jimenez del Toro, A., Teuwen, J. J. E., Tomás, F., & Finnegan, W. (2022). The Role of Melting on Intimate Contact Development in Laser-Assisted Tape Placement of Carbon Fibre Reinforced Thermoplastic Composites. In A. P. Vassilopoulos, & V. Michaud (Eds.), *Proceedings of the 20th European Conference on Composite Materials: Composites Meet Sustainability: Vol 2 – Manufacturing* (pp. 242-249). EPFL Lausanne, Composite Construction Laboratory.

Important note
To cite this publication, please use the final published version (if applicable).
Please check the document version above.

ECCM 20

26–30 JUNE 2022

LAUSANNE SWITZERLAND

Proceedings of the 20th European Conference on Composite Materials

COMPOSITES MEET SUSTAINABILITY

Vol 2 – Manufacturing

Editors : Anastasios P. Vassilopoulos, Véronique Michaud

Proceedings of the 20th
European Conference on Composite Materials
ECCM20
26-30 June 2022,
EPFL Lausanne Switzerland

Edited By :

Prof. Anastasios P. Vassilopoulos, CCLab/EPFL
Prof. Véronique Michaud, LPAC/EPFL

Oraganized by:

Composite Construction Laboratory (CCLab)
Laboratory for Processing of Advanced Composites (LPAC)
Ecole Polytechnique Fédérale de Lausanne (EPFL)

Cover:

Swiss Tech Convention Center
© Edouard Venceslau - CompuWeb SA

Cover Design:

Composite Construction Laboratory (CCLab)
Ecole Polytechnique Fédérale de Lausanne (EPFL)
Lausanne, Switzerland

Disclaimer:

The ECCM20 organizing committee and the Editors of these proceedings assume no responsibility or liability for the content, statements and opinions expressed by the authors in their corresponding publication.

THE ROLE OF MELTING ON INTIMATE CONTACT DEVELOPMENT IN LASER-ASSISTED TAPE PLACEMENT OF CARBON FIBRE REINFORCED THERMOPLASTIC COMPOSITES

Alejandro Jiménez del Toro[a,b,*], Julie Teuwen[b], Tomas Flanagan[a], William Finnegan[c,d]

a: ÉireComposites – a.jimenezdeltoro@eirecomposites.com
b: Delft University of Technology – a.jimenezdeltoro@tudelft.nl
c: National University of Ireland Galway
d: SFI MaREI Centre for Energy, Climate and Marine

Abstract: *Laser-assisted tape placement (LATP) and thermoplastic composites (TPCs) pre-impregnated (prepreg) tapes are a promising combination of technologies, combining in-situ consolidation of the TPCs and the high degree of automation achievable with LATP. Laminate quality tends to decrease when increasing placement speed due to the shortening of heating and consolidation window. Such heating windows require high laser power to achieve the desired nip point temperature, which can hinder through-thickness temperature distribution within the incoming tape during the heating stage. The effect of placement speed, laser power and thermal conductivity model on the temperature and melt profile of tapes prior the compaction phase will be investigated through simulations for carbon fibre reinforced polyphenylene sulphide unidirectional tapes. Results show that significant through-thickness thermal gradients occur within a tape at high laser power; and the obtained gradients differ for each thermal conductivity model used.*

Keywords: laser-assisted tape placement; melting, heat transfer model; thermal conductivity; heating stage

1. Introduction

Laser-assisted automated tape placement (LATP) of carbon fibre (CF) reinforced thermoplastic composites (TCs) is a versatile technology with the potential to utilise the in-situ consolidation capabilities of TCs to bring one-step manufacturing of composite parts. The in-situ consolidation of the part is achieved by continuous bonding of the incoming tape to the substrate, in which the interface between the two heals and restores bulk-like properties[1]. Such properties are developed when a high degree of bonding is achieved; which results from the contribution of the degree of autohesion and intimate contact, D_{ic}. However, current in-situ consolidation in LATP is not a robust process.

Prior to autohesion, it is crucial to achieve a high degree of intimate contact. Current intimate contact development models[2,3] rely on resin squeeze flow to describe the flattening of the surface's asperities upon compaction, and are unable to successfully predict experimental D_{ic} measurements[4]. Recent work has revealed that tape's surfaces are heterogeneous and can have resin poor areas. Kok[5] found a logarithmic relationship between D_{ic} and the resin poor surface depth, achieving D_{ic} approximately to 1 when that depth was close to zero, meaning the surface was resin rich. This shows that contrary to what current D_{ic} models, due to resin poor surface areas, both squeeze and through-thickness percolation flow are relevant in D_{ic} development. Hence, since through-thickness resin flow is required, not only surface

temperature but also its distribution within the tape become relevant parameters to analyse in LATP.

To improve deposition rates, both placement speed and/or tape's fibre areal weight can be increased. Elevated placement speeds can lead to significantly reduced processing times and impose very elevated heating rates regardless of the tape's thickness. Time scales in the order of tens of milliseconds and heating rates well above 5 000 °C/s can be expected. Polymers are thermal insulators and composites' through-thickness thermal conductivity, k_z, is highly influenced by this fact[6], which could compromise the temperature distribution within a tape upon heating in such short processing times. Thermal conductivity, k, is a function of thermal diffusivity, α, density, ρ, and specific heat capacity, c_p, as per Eq.(1).

$$k = \alpha \rho c_p \ [\text{W/m·K}] \tag{1}$$

It is worth noticing that all these properties depend on temperature and porosity, among others[7]. For several neat polymers[8], including polyphenylene sulphide (PPS)[9], α decreases with temperature. Also, k_z for CF/PPS composite has been reported to decrease with temperature[10], whereas an increase with temperature has been identified for CF reinforced polyether-ether-ketone (CF/PEEK)[7]. Several models have been developed to predict k_z values in composites and some of them will be used in this work. Examples of LATP modelling of heat transfer in composites with constant[11] and temperature-dependent[12] values of k_z can be found.

Given the low k_z of composites and the rapid surface heating due to elevated placement speeds, thermal gradients within the tape might occur and hinder percolation flow and intimate contact development. The presence and influence on intimate contact development of these thermal gradients has not been studied yet. The aim of this work is to evaluate the presence of through-thickness thermal gradients within a tape during the heating phase, prior to consolidation, using different placement speeds, laser powers and k_z models, by means of a finite element model (FEM). The steps followed in the study are: (1) a laser source and CF/PPS unidirectional composite are modelled based on previously reported studies; (2) the thermal history and through-thickness temperature profile of a CF/PPS unidirectional tape heated up by a laser source at different placement speeds, laser powers and thermal conductivities is simulated by finite element method; (3) the influence of k_z on the simulation results is evaluated.

2. Numerical modelling methodology

The finite element model was performed in COMSOL Multiphysics® 5.6, using the Backward Differentiation Formula solver for a transient heat transfer problem in which a moving laser heat source passes over a static rectangle of CF/PPS unidirectional composite. The geometry used was a 150 mm length and 0.15 mm thick rectangle. A triangular mesh with a maximum element size of 7 µm was sufficiently refined to observe no significant difference in the simulation results. The laser source have been modelled following the irradiance distribution described by Grouve [11], which has been simplified to an skewed top hat distribution to mimic the effect of the laser losing sight of the tape as it rolls under the roller. The reflection from the substrate are not accounted for in this model, and the roller is considered transparent to the laser and at constant temperature. The initial tape, ambient and roller

temperatures are 293.15 K. The upper surface of the geometry receives the radiation from the laser, and loses energy by means of convection with the environment and radiation. The lateral surfaces lose energy by the same means as the upper one but do not receive heat input. The bottom surface is always in perfect contact with the roller and loses energy by conduction. All parameters regarding geometry, placement and laser are listed in Table 1. The matrix-reinforcement distribution is considered homogeneous throughout the composite and its properties are listed in Table 2.

Table 1. Placement and laser simulation parameters.

Property	Symbol	Units	Value
Sample length	s_l	cm	1.5
Sample thickness	s_t	mm	0.15
Laser power	L_p	kW	1, 3, 6
Laser length	L_l	mm	45
Laser width	L_w	mm	28
Laser shadow length	L_{shadow}	mm	3
Placement speed	S	mm/s	100, 400, 800
Time step	t_{step}	s	0.001

Table 2. Composite, PPS and CF material properties.

Property	Symbol	Units	Value
Composite surface emissivity[10]	ϵ	—	0.9
Composite absorptivity[11]	A	—	0.9
PPS molecular weight	M_w	kg/mol	1
PPS melting temperature	T_m	°C	298
PPS density[13]	ρ_m	kg/m^3	1300
CF density[14]	ρ_f	kg/m^3	1790
Specific heat capacity of PPS[13]	$c_{p,m}^{solid}(298\,\text{K})$	J/g·K	1100
Heat capacity change of PPS at T_g[15]	$\Delta c_{p,m,a}(T_g)$	J/g·K	0.27
CF specific heat capacity[14]	$c_{p,f}$	J/kg·K	$750 + 2.05 \cdot T[K]$
Fibre volume fraction	χ_f	—	0.55
CF/PPS-air heat transfer coeff.[10]	h_{air}	W/m^{2}K	2.5
CF/PPS-roller heat transfer coeff.[11]	h_{roller}	W/m^{2}K	100

The heat capacity of CF/PPS, c_p, as a function of temperature was calculated from the individual heat capacities of each component applying the rule of mixtures. The specific heat of PPS, $c_{p,m}$, results from the heat capacity of solid, $c_{p,\text{m}}^{\text{solid}}(T)$, and molten, $c_{p,\text{m}}^{\text{melt}}(T)$, PPS which were estimated as described elsewhere[16]. $c_{p,m}^{\text{melt}}(298\,\text{K})$ was estimated as $c_{p,m}^{\text{melt}}(298\,\text{K}) = c_{p,m}^{\text{solid}}(298\,\text{K}) + \Delta c_{p,m,a}(T_g)$. It is assumed that the heat capacity of the molten polymer is achieved above T_g. Both, CF, ρ_f, and PPS, ρ_m, densities are assumed constant and the composite density, ρ, results from applying the rule of mixtures. Values for thermal diffusivity of PPS, $\alpha_m(T)$, are based on Chukov's[13] experimental work. In the presented thermal model,

they are calculated by means of cubic spline interpolation from 25 to 250 °C, and considered constant outside that interval. Thermal conductivity of PPS, k_m, has been estimated by Eq. (1) , using $\alpha_m(T)$, ρ_m and $c_{p,m}$ previously described. The thermal conductivity of carbon fibre in the longitudinal, $k_{x,f}$, and transverse, $k_{y,f}$ and $k_{z,f}$, direction have been estimated as described elsewhere[14].

2.2 Composite thermal conductivity

In this work, the influence on the temperature distribution of a tape has been studied for four different k_z models for the CF/PPS composite. These models are listed in Table 3.

Table 3. Composite through-thickness thermal conductivity, k_z, model equations used in the present study.

Model	k_z [W/m·K]
Rule of mixtures[17]	$\dfrac{k_{z,f}k_m}{k_{z,f}\chi_m + k_m\chi_f}$
Halpin-Tsai[18]	$k_m\left(\dfrac{1+\zeta\eta\chi_f}{1-\eta\chi_f}\right), \eta = \dfrac{\left(k_{z,f}/k_m\right)-1}{\left(k_{z,f}/k_m\right)+\zeta}, \zeta = 1$
Linear[10]	$0.5 - 3.5 \cdot 10^{-4}T$
Constant[7]	0.72

3. Results

The presented simulation results have been obtained at the vertical middle section of the geometry, 0.75 cm, at the end of heating stage for each placement speed, including the laser shadow. The simulation times are therefore a function of the placement speed as: 555 ms ($S = 100$ mm/s), 138 ms ($S = 400$ mm/s) and 69 ms ($S = 80$ mm/s). The laser shadow length is kept constant at 3 mm, as defined in Table 1. To assess the validity of results of this study, they have been compared to those experimentally produced by Grouve[11] for CF/PPS composites. The order of magnitude of the simulations results seem to agree with the experimental observations.
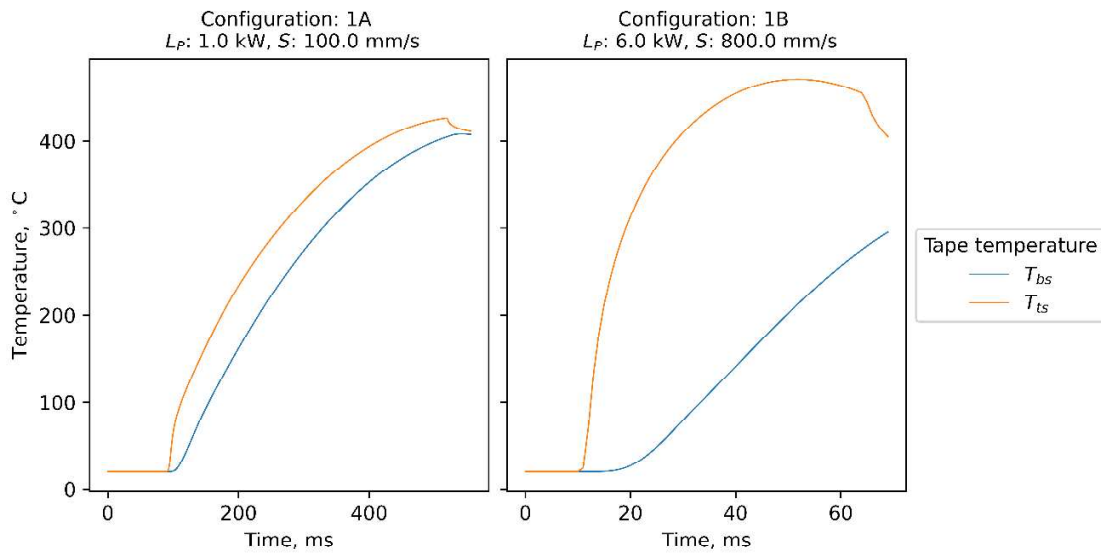
3.2. Laser power and placement speed effect on thermal history

As previously discussed, higher laser power is required for shorter heating times in order to achieve the desired temperatures, which leads to higher heating rates. The effect of the heating rates in the through-thickness temperature distribution, using Halpin-Tsai model for k_z calculation, can be observed in the solutions obtained for the configurations in Table 4 , shown in Figure 1. The temperature at the top surface (T_{ts}), which is heated by the laser, and the bottom surface (T_{bs}), which is on the opposite side of the tape, are evaluated at each time step during the heating phase for the middle section of the tape. An initial temperature plateau is seen before the laser reaches the middle section of the geometry, since $T_t = T_{ts} = T_{bs}$. Once the laser heats up the middle section, T_{ts} and T_{bs} increase differently as a function of L_P and k_z, generating a through-thickness temperature difference, $\Delta T_t = T_{ts} - T_{bs}$. As the tape enters the laser shadow region, a sudden temperature drop is experienced. Two ΔT_t are

of interest: $\Delta T_t^{end} = T_{ts}^{end} - T_{bs}^{end}$, which defines the through-thickness temperature difference at the end of the heating phase; and that between the maximum and final T_{ts}, $\Delta T_t^{drop} = T_{ts}^{max} - T_{ts}^{end}$, which represent the required tape superheating to achieve T_{ts}^{end}.

Table 4. Temperature evolution through the heating stage of the upper, T_{ts}, and bottom, T_{bs}, faces for two distinct LATP configurations: (1A) $L_P = 1.0$ kW and $S = 100$ mm/s; and (1B) $L_P = 6.0$ kW and $S = 800$ mm/s.

Configuration	L_P [kW]	S [mm/s]	Time [ms]	T_{ts}^{max} [°C]	ΔT_{ts}^{drop} [°C]	T_{ts}^{end} [°C]	T_{bs}^{end} [°C]	ΔT_t^{end} [°C]
1A	1.0	100	555	427	15	412	409	4
1B	6.0	800	69	471	66	405	296	109

Figure 1. Upper, T_{ts}, and bottom, T_{bs}, surface temperatures of a tape heated by (1A) a 1.0 kW laser at 100 mm/s; and (1B) a 6.0 kW laser at 800 mm/s.

Similar T_{ts}^{end} are estimated for these two laser power and placement speed configurations, 405 and 412 °C for configurations 1A and 1B, respectively. As expected, to reach similar temperatures higher heating rates are seen in configuration 1B, since the heating window is approximately 10 times shorter. ΔT_t^{end} changes significantly with the power of the heat source, from 4 to 109 °C for configurations 1A and 1B, respectively. In addition, T_{bs} is below 298 °C, the melting point of PPS, for configuration 1B. The superheating required to achieve similar final temperatures is greater for configuration 1B than 1A, 471 and 427 °C, respectively; which results in smaller ΔT_{ts}^{drop} for configuration 1A than 1B, 15 and 66 °C, respectively. The temperature drop for configuration 1A occurs right at the start of the laser shadow, whereas the drop for configuration 1B starts, with a lower slope, several milliseconds earlier.

3.2. Effect of k_z model on thermal history

The role of k_z on ΔT_t^{end}, being 0 μm the bottom surface and 150 μm the top surface heated by the laser, is shown in Figure 2. The melting line for PPS is plotted as temperature references.

All four k_z models used show different behavior as a function of the laser power. For configuration 2A, all models show similar ΔT_t^{end} except for the linear model, which predicts a higher value. In configuration 2B, all predictions show larger ΔT_t^{end} than in configuration 2A, being Halpin-Tsai and constant models the most moderate and closer to each other in their predictions; whereas the rule of mixtures and linear models show significantly wider temperature ranges. It is worth noticing that the linear model already predicts T_{bs}^{end} does not reach the melting temperature at the end of the laser shadow. For configuration 2C, the predicted ΔT_t^{end} has broaden up for all models and values considered. The linear model produces results with a T_{bs}^{end} below the melting line, respectively. The rule of mixture and Halpin-Tsai models show $T_{bs}^{end} < T_m$ too. The constant model is the only one predicting a full melt of the tape in configuration 2C. As the laser power increases from configuration 2A to 2C, the relative difference of T_{bs}^{end} and T_{ts}^{end} between the different models became larger as well.
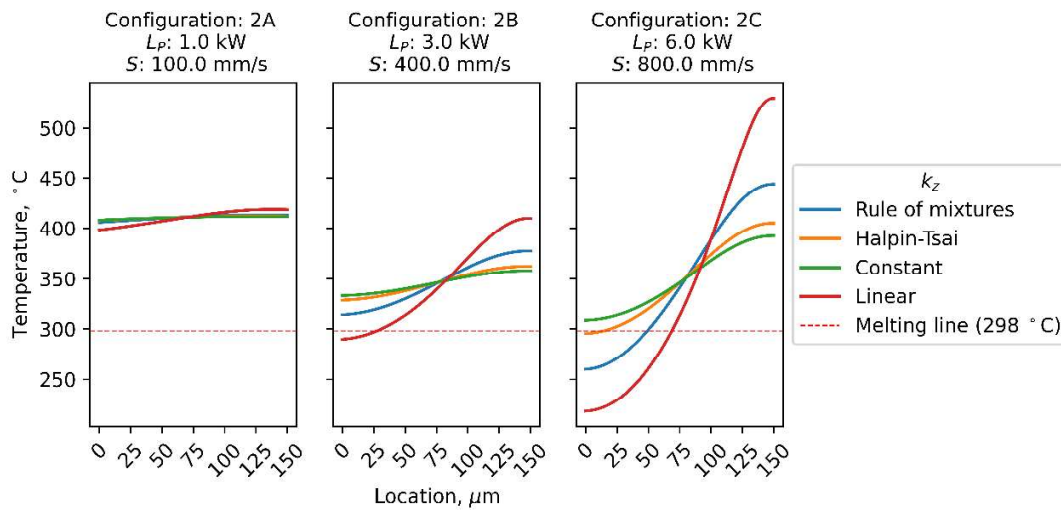

Figure 2. Estimated through-thickness temperature distribution (from the bottom surface, 0 μm, to the upper surface, 150 μm) at the end of the heating stage as a function of different k_z models for tapes heated up by (2A) a 1.0 kW laser at 100 mm/s, (2B) a 3.0 kW laser at 400 mm/s; and (2C) 6.0 kW laser at 800 mm/s.

4. Discussion

The simulated through-thickness thermal histories of a laser heated tape show results which depend on LATP configurations and k_z. Using Halpin-Tsai k_z model, as seen Figure 1, higher heating rates are produced to achieve similar T_{ts}^{end} as the placement speed and laser power increase; as a results, larger ΔT_t^{end}, ΔT_{ts}^{drop} and T_{ts}^{max} are experienced in the tape. Hence, choosing elevated nip point temperatures with high laser powers may produce polymer degradation upon heating. According to the simulations, this effect is not likely to occur at lower laser powers, since the tape superheating is not significant.

The effect of the LATP configuration and k_z model used on ΔT_t^{end} is shown in Figure 2. As laser power and heating rate increase, the larger ΔT_t^{end} becomes, which results in measurements of the tape's surface temperature not being representative of the actual tape through-thickness temperature. In fact, the rule of mixtures, Halpin-Tsai and the linear models

predict T_{bs}^{end} below T_m. This is not the case for low placement speeds, in which temperature homogenisation occurs prior compaction, as seen in Figure 2 (configuration 2A).

As the heating rates increase, the through-thickness temperature distributions obtained with the different k_z models also diverge from each other, as seen for the different configurations in Figure 2. Hence, the significant differences found between the k_z models as a function of the laser power make it necessary to experimentally determine the thermal conductivity to reach a higher confidence on the simulation results.

The existence of large through-thickness temperature distributions would also generate gradients in temperature dependent properties, such as viscosity and thermal expansion, among others. According to Darcy's law on percolation, it would hinder percolation towards the surface as the viscosity would increase from the heated surface into the tape. To the best of our knowledge, the effect of thermal gradients in the tape on the development of intimate contact has not yet been explored in literature

5. Conclusions

This work studied the development of through-thickness temperature gradients within a CF/PPS tape upon heating in LATP, as a function of different placement speeds and laser powers, by means of FEM analysis; as well as the influence of different k_z models on the obtained solutions. For all k_z models used, temperature gradients appear, and increase their value, as the laser power, and therefore heating rate, increase; some of them predict $T_{bs}^{end} < T_m$ for 6 kW laser power. For those configurations where through-thickness thermal gradients are present, readings of T_{ts} by means of a thermal camera would not represent the actual temperature of the tape. Different k_z models predict significantly different through-thickness temperature distributions for laser powers 3 and 6 kW; hence generating experimental data on this magnitude as a function of temperature seems necessary to improve the accuracy of the simulations. Resin flow may be hindered by the existence of thermal gradients within the tape thickness, which could be a negatively contributing factor to the development of intimate contact at high placement speeds.

Future work includes (1) the study of thermal history within a tape by experimental means, especially for elevated placement speeds; (2) the adequate characterisation of the composite properties as a function of temperature; (3) improvement and validation of the presented thermal model; (4) the possible role that the existence of thermal gradients might have on intimate contact development in LATP of CF/PPS composites.

Acknowledgements

6. References

1. Yassin K, Hojjati M. Processing of thermoplastic matrix composites through automated fiber placement and tape laying methods: A review. Journal of Thermoplastic Composite Materials. 2018 Dec;31(12):1676-725.
2. Lee WI, Springer GS. A model of the manufacturing process of thermoplastic matrix composites. Journal of composite materials. 1987 Nov;21(11):1017-55.

3. Yang F, Pitchumani R. A fractal Cantor set based description of interlaminar contact evolution during thermoplastic composites processing. Journal of materials science. 2001 Oct;36(19):4661-71.

4. Çelik O, Peeters D, Dransfeld C, Teuwen J. Intimate contact development during laser assisted fiber placement: Microstructure and effect of process parameters. Composites Part A: Applied Science and Manufacturing. 2020 Jul 1;134:105888.

5. Kok T. On the consolidation quality in laser assisted fiber placement: the role of the heating phase (Doctoral dissertation, University of Twente).

6. Tavman IH, Akinci H. Transverse thermal conductivity of fiber reinforced polymer composites. International Communications in Heat and Mass Transfer. 2000 Feb 1;27(2):253-61.

7. Cogswell FN. Thermoplastic aromatic polymer composites: a study of the structure, processing and properties of carbon fibre reinforced polyetheretherketone and related materials. Elsevier; 2013 Oct 22.

8. dos Santos WN, De Sousa JA, Gregorio Jr R. Thermal conductivity behaviour of polymers around glass transition and crystalline melting temperatures. Polymer Testing. 2013 Aug 1;32(5):987-94.

9. Dydek K, Latko-Durałek P, Sulowska A, Kubiś M, Demski S, Kozera P, Sztorch B, Boczkowska A. Effect of Processing Temperature and the Content of Carbon Nanotubes on the Properties of Nanocomposites Based on Polyphenylene Sulfide. Polymers. 2021 Jan;13(21):3816.

10. Y Carpier, Barbe F, B Vieille, A Coppalle. Identification of thermal properties and decomposition modelling of carbon fibers-PPS composites exposed to fire. In Proceeding of the 18th European Conference on Composite Materials (ECCM-18). ECCM, Athens, Greece. 2018. p. 24–8.

11. Grouve W. Weld strength of laser-assisted tape-placed thermoplastic composites (Doctoral dissertation, University of Twente).

12. Stokes-Griffin CM, Compston P, Matuszyk TI, Cardew-Hall MJ. Thermal modelling of the laser-assisted thermoplastic tape placement process. Journal of Thermoplastic Composite Materials. 2015 Oct;28(10):1445-62.

13. Chukov DI, Stepashkin AA, Tcherdyntsev VV, Olifirov LK, Kaloshkin SD. Structure and properties of composites based on polyphenylene sulfide reinforced with Al-Cu-Fe quasicrystalline particles. Journal of Thermoplastic Composite Materials. 2018 Jul;31(7):882-95.

14. Johnston AA. An integrated model of the development of process-induced deformation in autoclave processing of composite structures (Doctoral dissertation, University of British Columbia).

15. Wunderlich B. Thermal analysis of polymeric materials. Springer Science & Business Media; 2005 Apr 4.

16. Feldman D. Properties of polymers, by DW van Krevelen, Elsevier Science Publishers, Amsterdam, Oxford, New York, 1990, 875 pages, US $337.25. Journal of Polymer Science B Polymer Physics. 1991 Dec;29(13):1654-.

17. McCullough RL. Generalized combining rules for predicting transport properties of composite materials. Composites Science and Technology. 1985 Jan 1;22(1):3-21.

18. Affdl JH, Kardos JL. The Halpin-Tsai equations: a review. Polymer Engineering & Science. 1976 May;16(5):344-52.